CrystEngComm

Accepted Manuscript

ROYAL SOCIETY OF CHEMISTRY

www.rsc.org/crystengcomm

Journal Name

RSCPublishing

ARTICLE

From Monomers to Polymers: Steric and Supramolecular Effects on Dimensionality of Coordination Architectures in Heteroleptic Mercury(II) Halogenide – Tetradentate Schiff Base Complexes†

Cite this: DOI: 10.1039/xoxxoooooox

Received ooth January 2012,
Accepted ooth January 2012

DOI: 10.1039/xoxxoooooox

www.rsc.org/

Ghodrat Mahmoudi,[a,*] Vladimir Stilinovic,[b,*] Masoumeh Servati Gargari,[a] Antonio Bauzá[c], Guillermo Zaragoza[d], Werner Kaminsky,[e] Vincent Lynch,[f] Duane Choquesillo-Lazarte,[g] K. Sivakumar[h], Ali Akbar Khandar[i] and Antonio Frontera[c,*]

In this study, neutral mercury(II) complexes of composition $[Hg(\mathbf{L1})(\mu\text{-}Cl)_2Hg_3Cl_6]_n$ (**1**), $[Hg(\mathbf{L1})(\mu\text{-}Br)_2HgBr_2]$ (**2**), $[Hg(\mathbf{L3})Br_2]$ (**2a**), $[Hg(\mathbf{L1})I_2]$ (**3**), $[Hg(\mathbf{L2})Cl_2].CH_3OH$ (**4**) and $[Hg(\mathbf{L2})(\mu\text{-}Br)HgBr_3]_2$ (**5**) (**L1** = benzilbis((pyridin-2-yl)methylidenehydrazone; **L2** = benzilbis((acetylpyridin-2-yl)methylidenehydrazone) are described. Single-crystal X-ray crystallography showed that the molecular complexes can aggregate into larger entities depending upon the anion coordinated to the metal centre. Iodide gives discrete monomeric complexes; bromide generates 1D coordination polymer formed through Hg–Br–Hg bridges and chloride gives rise to an inorganic-organic hybrid material. The significant differences in the reaction conditions indicate that the anions exert a substantial influence on the formation of the compounds – smaller anions showing a larger potential for bridging between metal ions and forming coordination polymers. A minute increase in the bulkiness of the ligand (two extra methyl substituents in **L2**) dramatically changes the coordination architectures, and leads to formation of monomeric (chloride and iodide) and oligomeric (bromide), rather than polymeric structures. Noncovalent C–H/π and π–hole interactions observed in the solid state architecture of some complexes have been rationalized by means of theoretical DFT calculations.

1. Introduction

Construction of coordination networks by self-assembly has attracted considerable attention in crystal engineering and supramolecular chemistry, owing to versatile structural diversity and their potential applications in different areas from catalysis to nonlinear optics.[1-9] Factors that play an important role in controlling the architecture of self-assembled species include: the structure of ligands, the coordination geometry of metal ions, counter-anions, and supramolecular interactions of the coordination compound with its surroundings. Among these, anions play a very important role in the self-assembled construction.[17-24]

Due to their applications in paper industry and as preservatives, fluorescent lamps, sensors and batteries,[24-29] mercury and its compounds are of immense importance in chemistry and related disciplines. The spherical d^{10} configuration of Hg(II) is associated with a flexible coordination environment so that the geometries of these complexes can vary from linear to octahedral or even distorted hexagonal bipyramidal, and severe distortions from ideal coordination polyhedra occur easily. Furthermore, due to the lability of d^{10} metal complexes, the formation of coordination bonds is reversible, which enables metal ions and ligands to rearrange during the supramolecular assembly to allow the formation of the thermodynamically most stable structure, by varying the coordination polyhedron and coordination number of the mercury atom. Consequently, mercury(II) can readily accommodate different kinds of coordination frameworks, using a variety of organic ligands along with different inorganic/organic bridging units.[30]

In line with the above, we recently reported on the syntheses and the self-assembly of some Hg(II) compounds of composition $[Hg_2(\mu\text{-}L)(SCN)_4]_n$, $[Hg_2(\mu\text{-}L)(\mu\text{-}Cl)_2Cl_2]_n$, $[Hg_2(\mu\text{-}L)Br_4].[Hg_2(\mu\text{-}L)(\mu\text{-}Br)_2Br_2]_n$ and $[Hg_2(\mu\text{-}L)I_4]$ {L=*N*,*N*'-(bis-(pyridin-2-yl)benzylidene)-1,2-ethanediamine}.[31] Schiff base ligands are frequently used in coordination chemistry due to their significant ability to form stable complexes with metal ions.[32] The Schiff base ligand (L)

previously used by us[31a] played an important role in the formation of coordination polymers with fascinating structures. In this manuscript we investigate the effect of related azine-based Schiff base ligands (Scheme 1) on the solid state architecture of a series of Hg(II)-containing coordination compounds, namely $[Hg(\mathbf{L1})(\mu\text{-}Cl)_2Hg_3Cl_6]_n$ (**1**), $[Hg(\mathbf{L1})(\mu\text{-}Br)_2HgBr_2]$ (**2**), $[Hg(\mathbf{L3})Br_2]$ (**2a**), $[Hg(\mathbf{L1})I_2]$ (**3**), $[Hg(\mathbf{L2})Cl_2].CH_3OH$ (**4**) and $[Hg(\mathbf{L2})(\mu\text{-}Br)HgBr_3]_2$ (**5**) have been prepared by the reaction of a ligand (**L1** or **L2**) and HgX_2 (X = Cl, Br, I) in a 1 : 10 molar ratio. Herein, we report the structures and topological analyses of these compounds and discuss the influence of the anions on the structures of the coordination species. Moreover, the noncovalent C–H/π and π–hole interactions observed in the solid state architecture of some complexes have been rationalized by means of theoretical DFT calculations.

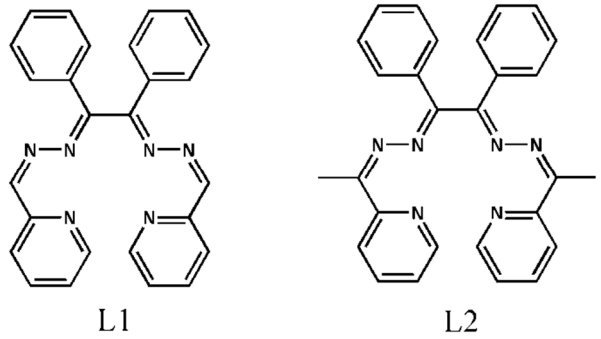

Scheme 1 Molecular diagrams of **L1** and **L2**.

2. Experimental methods

2.1. Materials and measurements

The ligands **L1** and **L2** were prepared following the reported method as described elsewhere[31b] and used without further purification. All other reagents and solvents used for the synthesis and analysis were commercially available and used as received. FT-IR spectra were recorded on a Bruker Tensor 27 FT-IR spectrometer. Microanalyses were performed using a Heraeus CHN-O-Rapid analyzer. Melting points were measured on an Electrothermal 9100 apparatus and are uncorrected.

Caution! Mercury and its compounds are toxic.[33] Only a small amount of these materials should be prepared and handled with care.

2.2. Synthesis of L1 and L2

Benzil dihydrazone (5.61 g, 23.58 mmol), was dissolved in 100 ml of anhydrous methanol. To this colourless solution, 4.50 ml (47.16 mmol) of freshly distilled 2-pyridinecarboxaldehyde was added. The resulting yellowish mixture was refluxed for 18 h, maintaining a dry atmosphere. Then it was slowly cooled to room temperature to yield yellowish crystalline solid, which was filtered off and dried in air. **L2** prepared same as **L1** except that 2-pyridinecarboxaldehyde was replaced by 2-acetyl pyridine.

2.3. Synthesis of $[Hg(L1)(\mu\text{-}Cl)_2Hg_3Cl_6]_n$ (1), $[Hg(L1)(\mu\text{-}Br)_2HgBr_2]$ (2), $[Hg(L1)I_2]$ (3), $[Hg(L2)Cl_2].CH_3OH$ (4) and $[Hg(L2)(\mu\text{-}Br)HgBr_3]_2$ (5)

Mercury(II) chloride and L1 (0.021 g, 0.05 mmol; 0.135 g, 0.5 mmol) were placed in the main arm of a branched tube. Methanol (10 ml) was carefully added to fill the arms. The tube was sealed and immersed in an oil bath at 60 °C while the branched arm was kept at ambient temperature. After 2 days, crystals of **1** that isolated in the cooler arm were filtered off, washed with acetone and ether, and dried in air. Crystals of **2** and **3** were prepared by a similar synthetic procedure to that used for **1**, except that $HgCl_2$ was replaced by $HgBr_2$ and HgI_2 respectively. For **4** and **5** a similar synthetic procedure to that used for **1** and **2** was used except that **L1** was replaced by **L2**. It is interesting to note that in all these cases an excess amount of HgX_2 (X = Cl, Br and I) was used – all attempts to prepare crystalline complexes in branched tube from equimolar mixtures were unsuccessful. For **1**: (0.157 g, yield 84%), found; (C, 20.68; H, 1.43; N, 5.67%. calcd. for $C_{26}H_{20}Cl_8Hg_4N_6$; C, 20.79 H, 1.37; N, 5.59%) IR (cm^{-1}) selected bands: 527(w), 687(vs), 776(vs), 973(m), 1155 (w), 1185(m), 1258(s), 1298(s), 1438(s), 1477(s), 1588(s), 1617(s), 3060(w). For **2**: (0.277 g, yield 74%), found; (C, 27.35; H, 1.83; N, 7.49%. calcd. for $C_{26}H_{20}Br_4Hg_2N_6$; C, 27.46 H, 1.77; N, 7.39%) IR (cm^{-1}) selected bands: 491(w), 625(m), 685(vs), 778 (m), 977(s), 1250(m), 1435(s), 1555(vs), 1613(m), 1651(m), 3060(w). For **3**: (0.295 g, yield 68%), found; (C, 35.75; H, 2.37; N, 9.76%. calcd. for $C_{26}H_{20}I_2HgN_6$; C, 35.86 H, 2.31; N, 9.65%) IR (cm^{-1}) selected bands: 527(w), 690(s), 776(m), 1058 (w), 1156(m), 1256(w), 1439(m), 1592(m), 1623(s), 3060(w). For 4: (0.205 g, yield 55%), found; (C, 46.44; H, 3.85; N, 11.35%. calcd. for $C_{29}H_{28}Cl_2HgN_6O$; C, 46.56 H,3.77; N, 11.23%) IR (cm^{-1}) selected bands: 574(w), 694(s), 780(s), 1003 (w), 1159(m), 1250(w), 1437(m), 1576(s), 1612(s), 3060(w). For 5: (0.118 g, yield 74%), found; (C, 28.75; H, 2.15; N, 7.28%. calcd. for $C_{28}H_{24}Br_4Hg_2N_6$; C, 28.86 H, 2.08; N, 7.21%) IR (cm^{-1}) selected bands: 566(w), 692(s), 778(m), 1010 (w), 1157(m), 1250(w), 1435(m), 1592(m), 1620(s), 3059(w).

2.4. Synthesis of $[Hg(L3)Br_2]$ (2a)

To a solution of benzilbis((pyridin-2-yl)methylidenehydrazone) (0.021 g, 0.05 mmol) in methanol (50 mL) a solution of $HgBr_2$ (0.18 g, 0.5 mmol) in methanol (40 mL) was added drop-wise under stirring, which resulted in the immediate formation of a yellow precipitate. Stirring was continued for 5 h and then the mixture was filtered. The residue was washed with methanol (3 × 10 mL) and dried under vacuum. The dried solid was dissolved in boiling in acetonitrile (45 mL) and filtered while hot. The filtrate, upon cooling to room temperature, afforded a yellow crystalline material (0.193 g, yield 44%), found; (C,46.35; H,2.93; N, 8.09%. calcd. for $C_{34}H_{25}Br_2HgN_5O$; C, 46.41 H,2.86; N, 7.96%) IR (cm^{-1}) selected bands: 688(m), 772(m), 1011(m), 1158 (m), 1385(s), 1437(m), 1565 (m), 1588(m), 1616(m), 1672(m), 3026(w).

2.5. X-ray crystallography

Table 1 Crystal and structure refinement data for prepared compounds

	1	**2**	**2a**	**3**	**4**	**5**	**L1**	**L2**
Chemical formula	$C_{26}H_{20}N_6Hg_4Cl_8$	$C_{26}H_{20}N_6Hg_2Br_4$	$C_{34}H_{25}N_5OHgBr_2$	$C_{26}H_{20}N_6HgI_2$	$C_{29}H_{28}N_6OHgCl_2$	$C_{56}H_{48}N_{12}Hg_4Br_8$	$C_{26}H_{20}N_6$	$C_{28}H_{24}N_6$
M_r	1502.44	1137.3	879.98	870.87	748.06	2330.63	416.48	444.53
Crystal system	triclinic	monoclinic	monoclinic	triclinic	triclinic	triclinic	monoclinic	triclinic
Space group	$P\bar{1}$	$P2_1/c$	$P2_1/n$	$P\bar{1}$	$P\bar{1}$	$P\bar{1}$	$P2_1/c$	$P\bar{1}$
a/Å	7.6970(3)	8.7552(8)	9.3733(7)	9.7571(6)	8.7640(4)	9.5360(4)	10.3079(4)	9.6825(15)
b/Å	15.9190(5)	14.1329(14)	35.998(2)	11.5338(8)	11.8787(4)	10.9904(4)	18.8288(7)	11.376(2)
c/Å	16.0270(7)	23.646(2)	9.8847(6)	14.2949(12)	15.0315(6)	15.8293(6)	11.5821(5)	12.377(2)
α/°	104.8910(10)	90	90	68.980(4)	73.615(3)	86.580(4)	90	74.062(3)
β/°	101.344(2)	96.847(5)	104.978(7)	83.774(4)	88.714(5)	73.062(3)	105.811(2)	76.504(4)
γ/°	99.190(4)	90	90	68.968(3)	88.110(6)	78.506(6)	90	66.011(3)
V/Å^3	1814.35(12)	2905.0(5)	3222.0(4)	1401.23(18)	1500.34(10)	1555.19(10)	2162.87(15)	1186.1(3)
Z	2	4	4	2	2	1	4	2
Z'	1	1	1	1	1	1/2	1	1
ρ_{calc}/(g cm^{-3})	2.75	2.6	1.814	2.064	1.656	2.489	1.279	1.245
μ/mm^{-1}	17.489	16.087	7.292	27.346	5.340	15.028	0.079	0.077
F[000]	1348	2072	1688	808	732	1068	872	468
Crystal size/mm^3	0.30×0.256×0.1	0.42×0.37×0.15	0.21×0.15×0.07	0.12×0.10×0.04	0.57×0.33×0.09	0.39×0.35×0.17	0.35×0.30×0.25	0.37×0.22×0.20
T / K	100(2)	100(2)	295(2)	296(2)	295(2)	295(2)	295(2)	100(2)
Reflections collected	12858	45335	27751	16554	11390	11042	26908	21324
Unique reflections	8150	5885	5631	4532	5181	5845	6510	5436
Observed reflections	4352	4451	2225	3030	4110	4466	3839	3895
Parameters	398	343	388	316	359	363	290	310
R_1(obs)	0.0787	0.0395	0.0323	0.0922	0.0558	0.0357	0.0447	0.0387
wR_2(all)	0.2325	0.0859	0.0456	0.2643	0.1369	0.0983	0.1168	0.0863
S	0.964	1.03	0.681	1.032	1.025	1.057	1.010	1.033
Max./min $\Delta\rho$/(e/Å^3)	2.695/ −3.586	1.169/ −2.048	0.476 / −0.465	2.463/ −1.544	2.106 / −2.964	1.363 / −1.786	0.190 / −0.138	0.222 / −0.18

The diffraction data were collected on a Nonius KappaCCD (**1**, 100 K, λ =0.71073 Å), Bruker APEX II (**2** and **2a**, 100 K, λ =0.71073 Å), Bruker X8 Proteum (**3**, 296 K, λ = 1.54178 Å) and Oxford Diffraction Xcalibur Kappa CCD (**4** and **5**, 295 K, λ =0.71073 Å) X-ray diffractometer. Data were processed with HKL Scalepack (**1**),[34] Apex2 (**2**, **2a**, **3**)[35] and CrysAlisPro (**4** and **5**)[36] programs and corrected for absorption using SADABS.[37] The structures were solved by direct methods,[38] which revealed the position of all non-hydrogen atoms. These atoms were refined on F^2 by a full-matrix least-squares procedure using anisotropic displacement parameters.[38] All hydrogen atoms were located in difference Fourier maps and included as fixed contributions riding on attached atoms with isotropic thermal displacement parameters 1.2 times those of the respective atom. All calculations were performed and the drawings were prepared using WINGX crystallographic suite of programs.[39] The crystal data are listed in Table 1. Further details are available from the Cambridge Crystallographic Centre – CCDC 1046009-1046016 contain the supplementary crystallographic data for **1-5**, **2a**, **L1** and **L2**

2.6. Theoretical methods

The geometries of the complexes included in this study were computed at the BP86-D3/def2-TZVP level of theory using the crystallographic coordinates within the TURBOMOLE program.[40] This level of theory that includes the latest available dispersion correction (D3) is adequate for studying non covalent interactions dominated by dispersion effects like π-stacking. The basis set superposition error for the calculation of interaction energies has been corrected using the counterpoise method.[41] The "atoms-in-molecules" (AIM)[42] analysis of the electron density has been performed at the same level of theory using the AIMAll program.[43]

3. Results and discussion

3.1. Synthesis and spectroscopic results

Ligands L1 and L2 were synthesized by refluxing benzil-dihydrazone with the corresponding aldehyde/keton in alcohol, according to the well-known condensation reaction between a primary amine and a ketone. The yields were almost quantitative in all cases. The reaction of equimolar amounts of these ligands and HgX_2 (X = Cl, Br and I) in methanol gave the corresponding complexes. However, single crystals could only be obtained if a tenfold excess of HgX_2 was used.

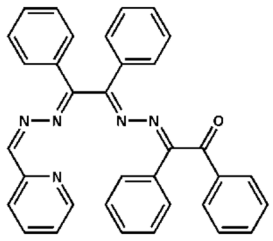

L3

Scheme 2 Molecular diagram of **L3**.

An original attempt to produce single crystals of **2** using an equimolar mixture of reactants failed and an attempt was made as described in Section 2.4. This however yielded an

unexpected product **2a**. Apparently this procedure led to partial hydrolysis of the ligand **L1**. This hydrolysis must have yielded several products among which probably were benzil and asymmetric benzyl-hydrazone-((pyridin-2-yl)methylidenehydrazone). The condensation of these two intermediates would then produce ligand **L3** (Scheme 2) which was detected in the crystal structure of **2a**.

The IR spectra of **1-5** exhibit ν(C=N) + ν(C=C) stretching vibrations [44] in the range 1650-1560 cm^{-1}, characteristic of metal bound imines.

3.2. Crystal structures of 1–5

Single crystal X-ray diffraction studies of all six coordination compounds **1**–**5** were made. All the bond lengths and angles in the ligands have the usual values for coordinated imines. [45, 46] ORTEP representations of molecules of **1**–**5** and perspective views of structural motifs in the crystal structures are shown in Figs. 1–8.

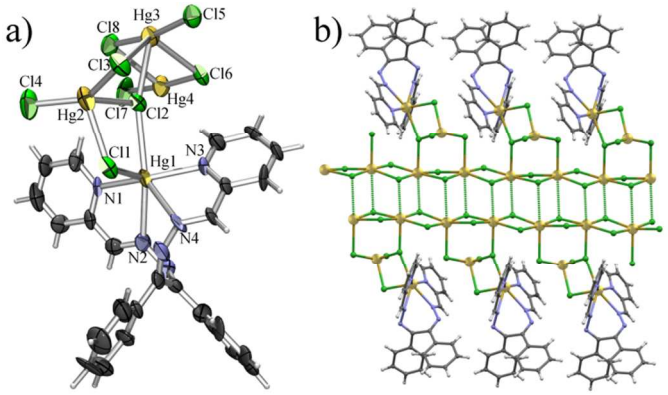

Fig. 1 a) ORTEP plot of a monomeric unit of **1** with the labelling of the metal and donor atoms. Thermal ellipsoids are shown at 50% probability and hydrogen atoms are shown as small spheres of arbitrary radii. b) A section of the polymeric double chain in the structure of **1**.

Single crystal diffraction experiments have shown **1** to be a 1D coordination polymer. The monomeric unit of the polymer comprises four symmetrically independent mercury(II) cations interconnected by bridging chloride anions. The polymeric structure is achieved through chains of $HgCl_2$ units along the crystallographic *a* axis which are further garnished with Hg_2Cl_4**L1** units comprising a $HgCl_4$ tetrahedron to which a terminal Hg**L1** is bonded (Fig. 1a). The two symmetrically independent mercury atoms which form the backbone of the coordination polymer (Hg3 and Hg4) have a distorted octahedral coordination with two short (ca. 2.3 Å) and two long Hg–Cl bonds (ca. 3.0 Å) forming the $(HgCl_2)_n$ chain, and two long Hg–Cl bonds of which one (2.82 Å and 2.95 Å) binds the Hg atoms of the chain with the $HgCl_4$ tetrahedra, while the substantially longer other one (3.25 Å and 3.60 Å) binds the Hg atoms of one $(HgCl_2)_n$ chain with bridging chlorides of a neighbouring one (Fig. 1b). The $HgCl_4$ tetrahedra formed about mercury atoms Hg2 are disphenoidally distorted with two shorter bonds with a terminal chloride (Hg2-Cl4 of 2.33 Å), and with a chloride bridging to the $(HgCl_2)_n$ chain (Hg2-Cl3 of 2.40 Å), and two longer bonds with chlorides bridging to the terminal mercury Hg1 cation (Hg2–Cl1 of 2.70 Å and Hg2–Cl2 of 2.68 Å) of which one (Cl2) also bridges to the $(HgCl_2)_n$ chain. The coordination of the terminal mercury ion can be described as heavily distorted trigonal prism with two chloride anions and N1 of the ligand **L1** as vertices of one base and N2, N3 and N4 vertices of the other. Of the Hg–N bonds, the bonds with the pyridine nitrogen atoms are markedly shorter (Hg1–N1 of 2.21 Å and Hg1–N3 of 2.26 Å) than those with imine nitrogen atoms (Hg1–N2 of 2.60 Å and Hg1–N4 of 2.47 Å). The molecule of **L1** is helically twisted to encompass Hg1 atom so that the ligand molecule assumes a conformation of approximate *C*2 symmetry.

Compound **2**, formed when chloride was replaced with bromide, was also found to be a coordination polymer. Here however the monomeric unit comprises only two symmetrically independent mercury(II) cations, each bonded to two bromides which acted as bridges between mercury cations forming a polymer along the crystallographic *b* axis (Fig. 2). One of the mercury cations (Hg2) is a centre of a $HgBr_4$ tetrahedron, which is again disphenoidally distorted with two shorter bonds with terminal bromides (Hg2–Br3 of 2.45 Å and Hg2–Br4 of 2.46 Å), and two longer bonds with bridging bromides (Hg2–Br1 of 2.82 Å and Hg2–Br2 of 2.86 Å). The coordination of the other mercury cation (Hg1) is similar to that of Hg1 in **1** with two bridging bromides and a tetracoordinating **L1**. Here however all the Hg–N bonds are of similar lengths (in the range 2.42 Å to 2.55 Å), and the overall coordination polyhedron is an intermediate between a (distorted) octahedron and a (distorted) trigonal prism.

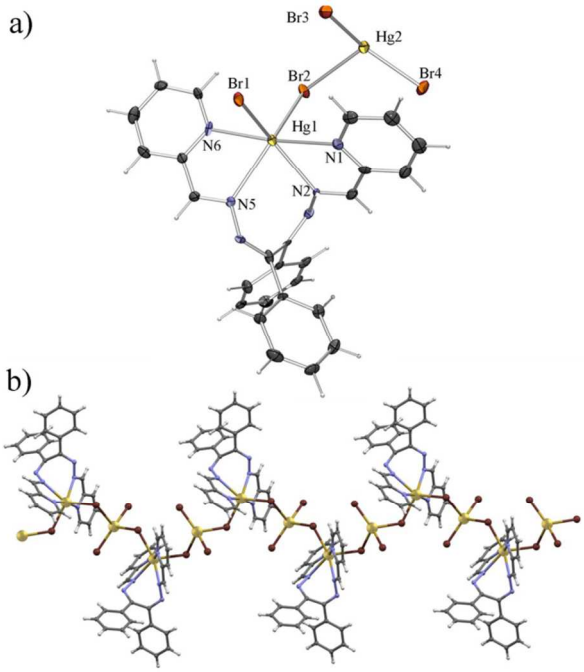

Fig. 2 a) ORTEP plot of a monomeric unit of **2** with the labelling of the metal and donor atoms. Thermal ellipsoids are shown at 50% probability and hydrogen atoms are shown as small spheres of arbitrary radii. b) A section of the polymeric chain in the structure of **2**.

Although structurally quite different from the chloride **1**, the bromide derivative was found to be isostructural with a previously described chloride analogue[32] (see Fig. S1) from which it only differs due to the larger Hg–Br bond lengths as compared to the Hg–Cl bonds, which subsequently leads also to an increase in the length of *b* axis, as compared to the isostructural chloride.

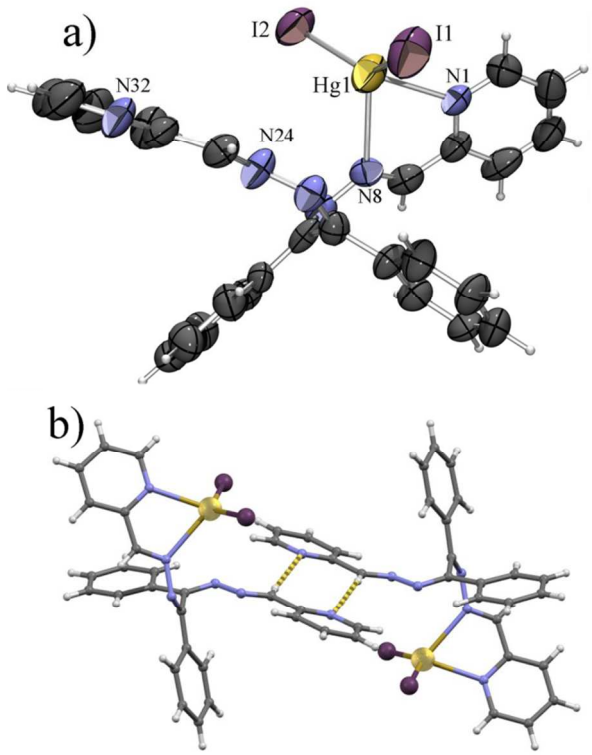

Fig. 3 a) ORTEP plot of a molecule of **3** with the labelling of the metal and donor atoms. Thermal ellipsoids are shown at 50% probability and hydrogen atoms are shown as small spheres of arbitrary radii. b) A C-H···N hydrogen bonded dimer in the structure of **3**.

Introduction of iodide, in place of the chloride or bromide, leads to a significant change in the molecular structure. Unlike **1** and **2**, that are polymeric, the iodide derivative **3** was found to be a mononuclear complex. Also, **L1** is in this case only bidentate, chelating mercury(II) with only one pyridine and one imine nitrogen atom. This makes the mercury ion tetrahedraly coordinated with the two nitrogen atoms and two iodide anions (Fig. 3a). This $HgI_2[N]_2$ tetrahedron shows even larger disphenoidal distortion, not so much due to the difference in Hg–I (Hg1–I1 of 2.64 Å and Hg1–I2 of 2.65 Å) and Hg–N bond lengths (Hg1–N1 of 2.45 Å and Hg1–N3 of 2.56 Å), but to a large difference between the chelate bite angle (φ(N1–Hg1–N2) = 67.0°) and the I1–Hg1–I2 angle (φ(I1–Hg1–I2) = 135.4°) due to the large Van der Waals radius of the iodide (non bonded I···I distance of 4.46 Å). The large Van der Waals radius of iodide is also the probable cause of the change of the coordination mode of **L1** which due to the increased size of the halogen can no longer act as a tetradentate ligand due to sterical hindrance. The molecular structure is almost identical to that reported for the HgI_2**L2** complex,[47] with minor differences in the conformation of the ligand molecule, most ostensively in the non-chelating arm of the ligand. These differences are likely caused by the different supramolecular environment – the azomethine CH group of the uncoordinated arm of **L1** forms a hydrogen bond with a pyridine nitrogen of a neighbouring molecule (C26–H26···N32 of 3.60 Å) closing a centrosymmetric R_2^2 (8) motif (Fig. 3b). Such C–H···N hydrogen bond, which is often a significant interaction in imines derived from pyridine,[48] is not possible in the case of **L2**, as there the azomethyne hydrogen has been replaced by a methyl group.

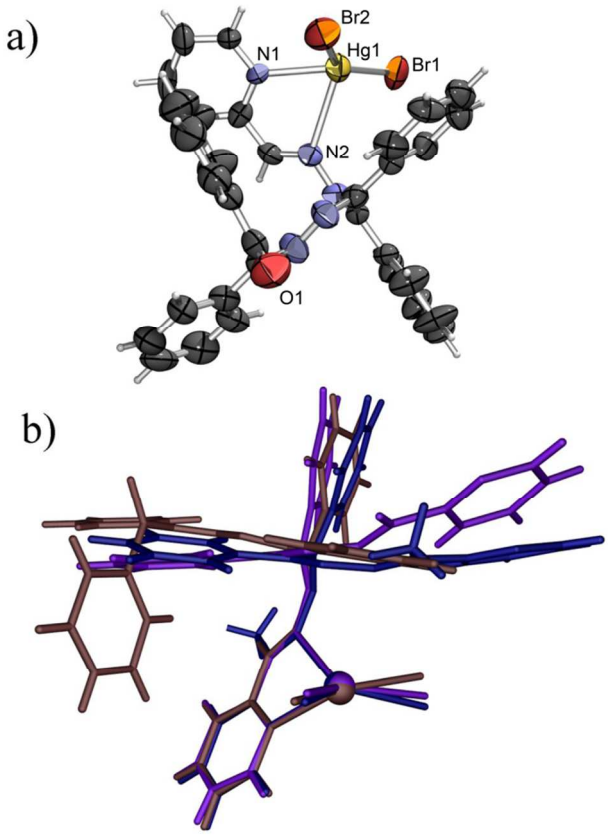

Fig. 4 a) ORTEP plot of a molecule of **2a** with the labelling of the metal and donor atoms. Thermal ellipsoids are shown at 50% probability and hydrogen atoms are shown as small spheres of arbitrary radii. b) Overlap of the molecules of **2a** (brown), **3** (violet) and HgI_2**L2** (blue) showing the overall similarity of the three molecules. The chelate ring atoms have been chosen as anchor atoms for the overlap.

The steric effect on the coordination of the ligand to mercury(II) halogenides is also demonstrated by **2a** ($HgBr_2$**L3**), where mercury is coordinated by two bromides and an organic ligand derived from **L1** by replacing one 2-pyridil group with a benzyl and a phenyl ring, rendering it far bulkier (Fig. 4a). Not only is the coordination polyhedron of the cation here almost identical to that in the iodide complexes, being a disphenoidally distorted tetrahedron with similar Hg–Br (Hg1–Br1 of 2.45 Å and Hg1–Br2 of 2.49 Å); and Hg–N bond lengths (Hg1–N1 of

2.38 Å and Hg1–N2 of 2.70 Å) while the angle between terminal Hg-Br bonds (φ(Br1–Hg1–Br2) = 142.0°) is much larger than the chelate angle (N1–Hg1–N2) = 66.7°), but the general shape of the molecule is quite similar to the shapes of **3** and HgI_2**L2** molecules (Fig. 4b).

Unlike in the case of the iodide complex where the replacement of **L1** with its dimethyl derivative **L2** does not lead to any significant change in coordination or molecular geometry, both the mercury(II) chloride and the bromide complexes obtained with **L2** have been found to be quite different then the respective **L1** complexes.

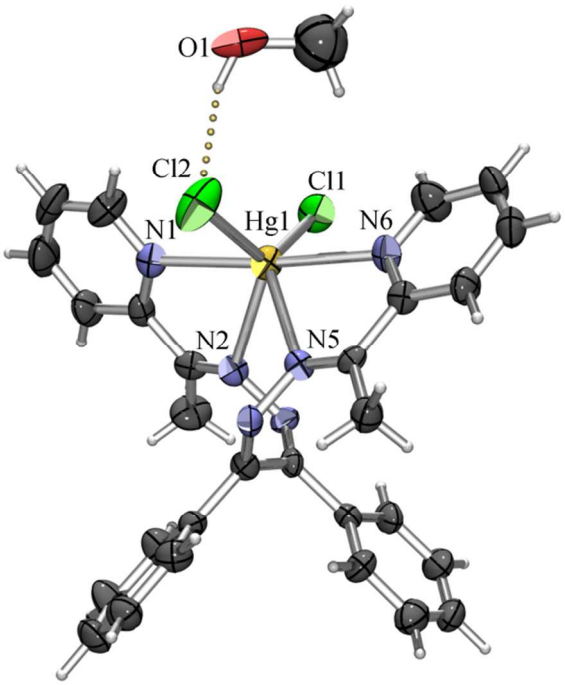

Fig. 5 ORTEP plot of an asymmetric unit of **4** with the labelling of the metal and donor atoms. Thermal ellipsoids are shown at 50% probability and hydrogen atoms are shown as small spheres of arbitrary radii.

The chloride derivative **4** is a monomeric specie found to crystallise as a methanol solvate. The coordination of the mercury(II) ion is similar to one of the terminal Hg1 in the structure of **1**, the with the four nitrogen atoms of the tetradentate **L2** and two chloride anions defining vertices of a highly irregular polyhedron (intermediate between a octahedron and a trigonal prism). Unlike in **1**, however, all the Hg–N bonds are of similar lengths (in the 2.50 Å to 2.57 Å range), and the Hg–Cl bonds are considerably shorter (Hg1–Cl1 of 2.44 Å and Hg1–Cl2 of 2.47 Å) than those in **1**, which is only to be expected as here the chlorides are not shared with another mercury cation. The slight difference in length of the two Hg–Cl bonds can be brought into connection with intermolecular hydrogen binding. As noted earlier, **4** crystallised as a methanol solvate, and the methanol molecule is hydrogen bonded to one coordinated chloride (O1–H1o···Cl2 of 3.14 Å), which can be assigned as a reason for slight stretching of the Hg1–Cl2 bond (Fig. 5). By binding to a coordinated chloride, the methanol molecule blocks it from forming other interactions, and thus prevents the chloride to act as a bridge towards another mercury atom. Therefore, although **L2** is a slightly sterically more demanding than **L1**, it cannot be maintained that the absence of polymerisation in this case is due to the change of the ligand. Rather, the supramolecular environment (i.e. hydrogen bonding of the coordinated chloride) which prevents the formation of chloride bridges appears to be a more likely cause of the monomeric nature of **4**.

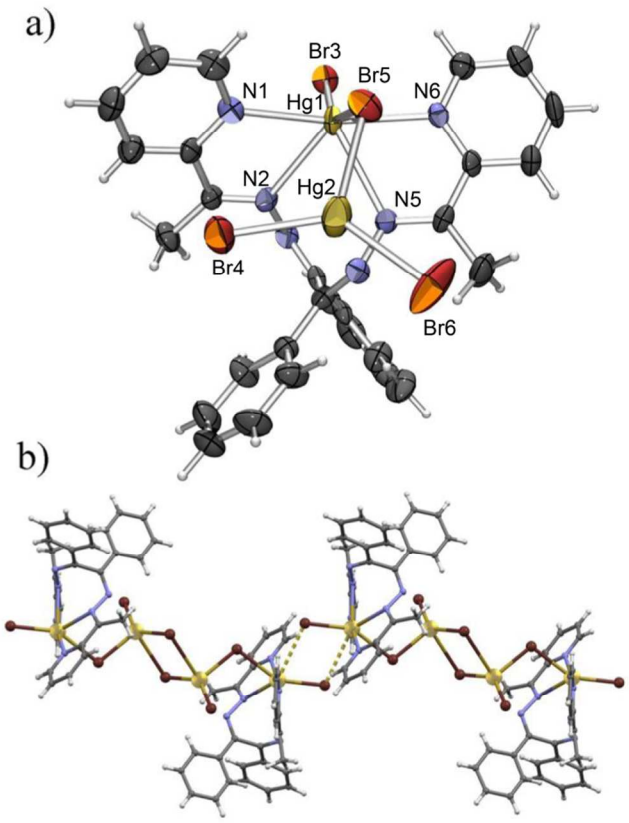

Fig. 6 a) ORTEP plot of a monomeric unit of **5** with the labelling of the metal and donor atoms. Thermal ellipsoids are shown at 50% probability and hydrogen atoms are shown as small spheres of arbitrary radii. b) Tetranuclear molecules of **5** interconnecting into chains by weak Hg-Br interactions.

The latter conclusion is to an extent justified by the structure of the bromide derivative **5**, which was found to be a tetranuclear complex with bridging bromides. This complex consists of two Hg_2Br_4**L2** monomeric units, equivalent to those forming the polymer **2**, although of a different conformation (Figs. 6a and 7). Unlike in **2**, however these units bind in a head-to-head manner into a centrosymetric dimer. The resulting complex molecule thus comprises of two terminal HgBr**L2** units and two $HgBr_4$ tetrahedra with a common edge (consisting of two Hg4 atoms related by an inversion centre) which bridge between them. The $HgBr_4$ tetrahedra are extremely distorted with the Hg2 atom almost coplanar with Br2, Br3 and Br4 (elevated from the Br2–Br3–Br4 plane by only 0.13 Å) to which it binds with short bonds (Hg2–Br2 of 2.62 Å, Hg2–Br3 of 2.47 Å and Hg2–Br4 of 2.48 Å), and with a very long bond (Hg2–Br4 of 3.24 Å) to the other Br4. The coordination of the terminal Hg1

cation is quite similar to the one described in **2**, with similar Hg–N bond lengths (in the range 2.40 Å to 2.58 Å), although with a large difference between the terminal (Hg1–Br1 of 2.64 Å) and the bridging Hg–Br (Hg1–Br2 of 2.86 Å) bonds. The Br1–Hg1–Br2 angle is also significantly larger (φ(Br1-Hg1-Br2) = 150.4° in **5** as opposed to 110.9° in **2**), although this can be attributed to the close proximity of Br1 from a neighbouring molecule which approaches Hg1 (Hg1···Br1' contact of 3.52Å) between the two coordinated bromides spreading them apart. This weak *quasi*-coordinative interaction interconnects the tetranuclear molecules into chains in the crystallographic [–1 0 1] direction (Fig. 6b).

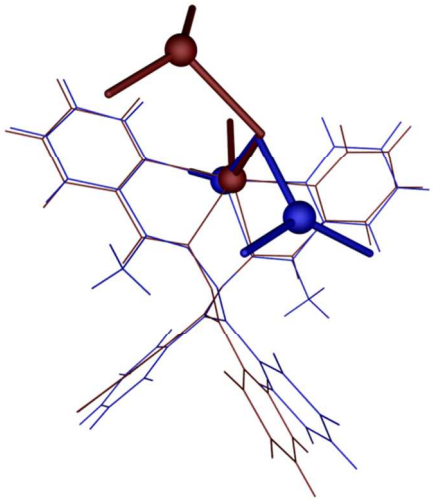

Fig. 7. Overlap of Hg_2Br_4**L** units in **2** (red) and **5** (blue). Mercury atoms are shown as small spheres. The chelated mercury atom and the chelating nitrogen atoms of the organic ligand have been chosen as anchor atoms for the overlap. Mercury atoms are shown as spheres and bromides as sticks.

3.5 Theoretical study of the supramolecular assemblies

We have focused the theoretical study to analyse the interesting supramolecular assemblies observed in the solid state of complexes **2a**, **3** and **4** (see Fig. 8). In complex **2a** we have analysed the C–H···π/π···π/π···H–C supramolecular assembly (see Fig. 8A) observed in the solid state. In **3** we have analysed a self-complementary dimer that is governed by two symmetrically related C7···N9 π-hole interactions. That is, the lone pair of the N9 atom interacts with the positive π-hole located at the carbon C7 atom of the imidic C=N bond (see Fig. 9B). This lp···π–hole interactions[49] are attracting increasing attention to the scientific community due to their important role in crystal engineering and supramolecular chemistry.[50] Finally, in compound **3** we have also analysed a self-assembled dimer where two complementary C–H···π interactions are established (see Fig. 8C).

The complexation energies of the selected crystallographic fragments are also included in Fig. 9. It can be observed that they are large and negative, indicating that they are strong binding motifs in the solid state structures. We have focused the theoretical study to analyze the influence of the complexation of the organic ligand to the Hg(II) metal centre on the strength of the noncovalent interactions. Therefore we have used several theoretical models based on the crystal structures. For compound **2a** we have used two models and the binding energies (Fig. 9) are compared to the corresponding one obtained for the crystallographic dimer shown in Fig. 8A.

We have first analysed the influence of the intramolecular C–H···π interaction on the binding energy of the dimer. Therefore we have used a model where the phenyl groups that participate in the C–H···π interactions have been replaced by hydrogen atoms (see arrows in Fig. 9A). As a result the binding energy (ΔE_4 = –16.4 kcal/mol) was slightly reduced compared to ΔE_1 = –16.7 kcal/mol (see Fig. 8A), therefore the influence of the C–

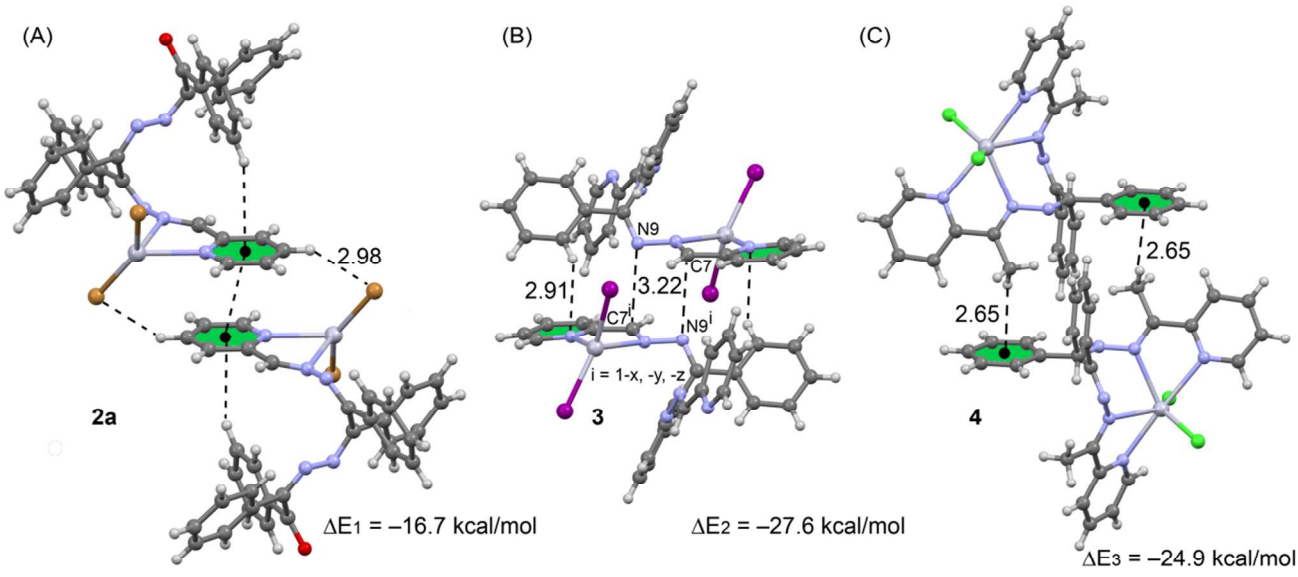

Fig. 8 Dimeric crystal fragments of compounds **2a**, **3** and **4** and their interaction energies.

H···π interaction on the strength of the π···π interaction is almost negligible. Secondly, we have analyzed the influence of the metal complexation on the binding energy by eliminating the $HgBr_2$ part of the molecule. By doing so, the interaction energy is significantly reduced to ΔE_5 = –7.0 kcal/mol that is the contribution of the π···π interaction to the supramolecular assembly. The difference between ΔE_1 and ΔE_5 corresponds to the contribution of both C–H···Br hydrogen bonds, that is $\Delta E_1 - \Delta E_5$.= –9.7 kcal/mol.

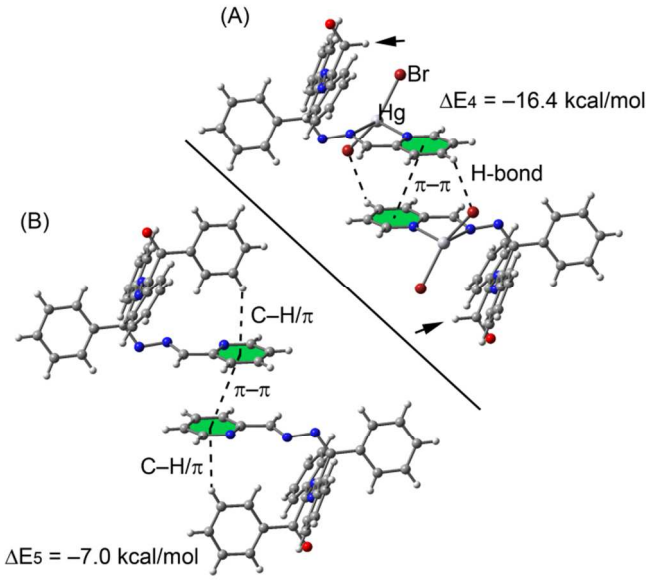

Fig. 9 Theoretical models used to evaluate the noncovalent interactions in compound **2a**.

The theoretical models used to analyse the contribution of the different noncovalent interactions in complexes **3** and **4** are shown in Fig. 10. For complex **3** we have used two models. In the first one we have replaced the phenyl groups that establish the C–H···π interaction by hydrogen atoms (see small arrows in Fig. 11A). As a result the interaction energy is reduced from ΔE_2 = –27.6 kcal/mol (see Fig. 8B) to ΔE_6 = –18.8 kcal/mol that corresponds to the interaction energy associated to the double π–hole interaction. Therefore each C–H···π interaction can be estimated as $(\Delta E_2 - \Delta E_6)/2$= –4.3 kcal/mol. In order to analyze the influence of the metal coordination on the π–hole interaction, we have used another theoretical model (see Fig. 11B) where the HgI_2 moieties have been eliminated. In this model the interaction energy is further reduced to ΔE_6 = –5.8 kcal/mol, indicating that the complexation of the imidic nitrogen atom to the Hg metal centre has a strong influence on the magnitude of the π–hole at the carbon atom. To corroborate this explanation, we have computed the atomic Mulliken charge at C7 carbon in the presence and absence of the HgI_2 moiety. As a result, the charge at the imidic carbon atom becomes 0.16 *e* more positive in the presence of the metal centre.

Finally, in complex **3** we have used a theoretical model to evaluate the influence of the metal complexation on the self-complementary CH_3···π interaction (see Fig. 10C). In this case the interaction energy in the absence of $HgCl_2$ is considerably reduced from ΔE_2 = –24.9 kcal/mol (see Fig. 8C) to ΔE_6 = –11.3 kcal/mol that corresponds to the interaction energy associated to the double CH_3···π interaction. A likely explanation for this significant reduction is that the acidity of the methyl hydrogen atom increases as a consequence of the complexation of the organic ligand to the Hg(II) ion.

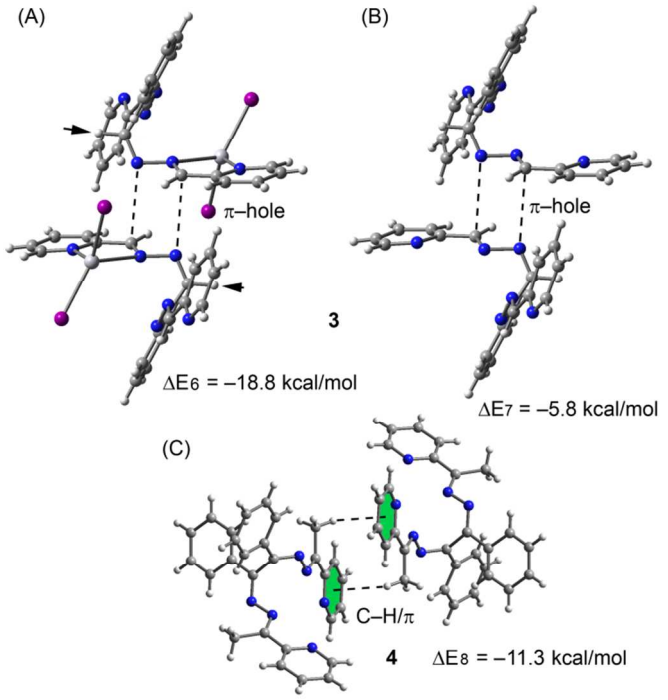

Fig. 10. Theoretical models used to evaluate the noncovalent interactions in compounds **3** (A and B) and **4** (C).

In order to characterize the noncovalent interactions explained above, we have used the Bader's "atoms-in-molecules" methodology[42] that provides an unambiguous definition of chemical bonding. The existence of a bond critical point and a bond path connecting two atoms can be used as a confirmation of covalent/noncovalent bonding. The AIM analyses of the theoretical models corresponding to compounds **2a**, **3** and **4** are shown in Figs. S2 and S3. All noncovalent interaction described above have been confirmed by the existence of several bond critical points and bond paths connecting the interacting atoms, see ESI for details.

4. Conclusions

In conclusion, we herein reported the syntheses and structural characterization of six new mercury(II) complexes **1**–**5** with halogenide and organic ligands, where a comparison between structurally similar ligands, L1 and L2, was made. Although the difference between the two ligands is minute (they differ only in presence/absence of two methyl groups) the choice of ligand has an immense effect on the coordination behaviour of mercury when bromide or chloride was the anionic ligand

present. This is related to the differences in the supramolecular assemblies formed by the complexes, which in turn affect the molecular packing. The simple addition of a methyl group to the ligand controls on one hand the formation of a dimer instead of a polymer (as in compound 5) and, on the other hand, the formation of supramolecular assemblies due to the participation in $CH_3\cdots\pi$ interactions, as demonstrated by the DFT analysis.

Acknowledgements

We are grateful to the University of Tabriz Research Council for the financial support of this research. The project "Factoría de Cristalización, CONSOLIDER INGENIO-2010" provided X-ray structural facilities for this work. AF and AB thank MINECO of Spain (project CONSOLIDER INGENIO 2010 CSD2010-00065, FEDER funds) and the CTI (UIB) for free allocation of computer time.

Notes and references

[a]*Young Researchers and Elite Club, Tabriz Branch, Islamic Azad University, Tabriz, Iran, E-mail: mahmoudi_ghodrat@yahoo.co.uk*
[b]*Department of Chemistry, Faculty of Science, University of Zagreb, Horvatovac 102a, HR-10000 Zagreb, Croatia*
[c]*Departament de Química, Universitat de les Illes Balears, Crta. de Valldemossa km 7.5, 07122 Palma de Mallorca (Baleares), SPAIN, E-mail: toni.frontera@uib.es*
[d]*Unidad de RX, Edificio CACTUS, Campus Vida, 15782 Santiago Compostela, Spain*
[e]*X-ray Crystallography Laboratory, University of Washington, USA*
[f]*Department of Chemistry and Biochemistry University of Texas at Austin, Austin, TX 78712, USA*
[g]*Laboratorio de Estudios Cristalográficos, IACT, CSIC-Universidad de Granada, Avda. de las Palmeras 4, 18100 – Armilla (Granada), Spain*
[h]*Department of Physics, Anna University, Chennai 600 025, India*
[i]*Department of Inorganic Chemistry, Faculty of Chemistry, University of Tabriz, P.O. Box 5166616471, Tabriz, Iran*

CCDC 1046009-1046016 contain the supplementary crystallographic data for **1-5, L1** and **L2**. These data can be obtained free of charge via http://www.ccdc.cam.ac.uk/conts/retrieving.html, or from the Cambridge Crystallographic Data Centre, 12, Union Road, Cambridge CB2 1EZ, UK; Fax: (+44) 1223-336-033; or e-mail: deposit@ccdc.cam.ac.uk.

† Electronic supplementary information (ESI) available: Fig.s S1–S3 and the AIM results and discussion.

1 K. Y. Wang, L. J. Zhou, M. L. Feng and X. Y. Huang, *Dalton Trans*., 2012, **41**, 6689–6695.
2 S. Kitagawa, R. Kitaura and S. Noro, *Angew. Chem., Int. Ed*., 2004, **43**, 2334–2375.
3 C. S. Liu, X. S. Shi, J. R. Li, J. J. Wang and X. H. Bu, *Cryst. Growth Des*., 2006, **6**, 656–663.
4 S. G. Telfer and R. Kuroda, *Coord. Chem. Rev*., 2003, **242**, 33–46.
5 S. A. Barnett and N. R. Champness, *Coord. Chem. Rev*., 2003, **246**, 145–168.
6 C. D. Wu, A. G. Hu, L. Zhang and W. B. Lin, *J. Am. Chem. Soc.*, 2005, **127**, 8940–8941.
7 B. Moulton and M. J. Zaworotko, *Chem. Rev*., 2001, **101**, 1629–1658.
8 L. C. Tabares, J. A. R. Navarro and J. M. Salas, *J. Am. Chem. Soc.*, 2001, **123**, 383–387.
9 Y. Zhao, Z. Lin, H. Wu and C. Duan, *Inorg. Chem*., 2006, **45**, 10013–10015.
10 H. R. Khavasi, A. R. Salimi, H. Eshtiagh-Hosseini and M. M. Amini, *CrystEngComm*, 2011, **13**, 3710–3717.
11 I. Kuzu, I. Krummenacher, J. Meyer, F. Armbruster and F. Breher, *Dalton Trans*., 2008, 5836–5865.
12 C. Janiak, *J. Chem. Soc., Dalton Trans*., 2000, 3885–3896.
13 S. Re and S. Nagase, *Chem. Commun*., 2004, 658–659; B. H. Northrop, Y. R. Zheng, K. W. Chi and P. J. Stang, *Acc. Chem. Res*., 2009, **42**, 1554–1563.
14 C. J. Elsevier, J. Reedijk, P. H. Walton and M. D. Ward, *Dalton Trans*., 2003, 1869–1880.
15 B. Olenyuk, A. Fechtenkötter and P. J. Stang, *J. Chem. Soc., Dalton Trans*., 1998, 1707–1728.
16 G. S. Papaefstathiou and L. R. MacGillivray, *Coord. Chem. Rev*., 2003, **246**, 169–184.
17 H.-P. Zhou, X.- P. Gan, X.-L. Li, Z.-D. Liu, W.-Q. Geng, F.-X. Zhou, W.-Z. Ke, P. Wang, L. Kong, F.-Y. Hao, J.-Y. Wu and Y.-P. Tian, *Cryst. Growth Des*., 2010, **10**, 1767–1776.
18 H.-P. Zhou, J.-H. Yin, L.-X. Zheng, P. Wang, F.-Y. Hao, W.-Q. Geng, X.-P. Gan, G.- Y. Xu, J.-Y. Wu, Y.-P. Tian, X.-T. Tao, M.-H. Jiang and Y.- H. Kan, *Cryst. Growth Des*., 2009, **9**, 3789–3798.
19 S. Y. Lee, S. Park, H. J. Kim, J. H. Jung and S. S. Lee, *Inorg. Chem*., 2008, **47**, 1913–1915.
20 B. L. Schottel, H. T. Chifotides, M. Shatruk, A. Chouai, L. M. Perez, J. Bacsa and K. R. Dunbar, *J. Am. Chem. Soc.*, 2006, **128**, 5895–5912.
21 C. S. Campos-Fernandez, B. L. Schottel, H. T. Chifotides, J. K. Bera, J. Bacsa, J. M. Koomen, D. H. Russell and K. R. Dunbar, *J. Am. Chem. Soc.*, 2005, **127**, 12909–12923.
22 F. Zeng, J. Ni, Q. Wang, Y. Ding, S. W. Ng, W. Zhu and Y. Xie, *Cryst. Growth Des*., 2010, **10**, 1611–1622.
23 P. Manna, S. K. Seth, A. Das, J. Hemming, R. Prendergast, M. Helliwell, S. R. Choudhury, A. Frontera and S. Mukhopadhyay, *Inorg. Chem*., 2012, **51**, 3557–3571.
24 V. Stilinović, K. Užarević, I. Cvrtila and B. Kaitner, *CrystEngComm*, 2012, **14**, 7493–7501.
25 K. Huber, Wisconsin Mercury Source Book, Wisconsin Department of Natural Resources, Bureau of Watershed Management, Madison, WI, 1997.
26 M. F. Hawthorne and Z. Zheng, *Acc. Chem. Res*., 1997, **30**, 267–276.
27 A. Tamayo, B. Pedras, C. Lodeiro, L. Escriche, J. Casabo, J. L. Capelo, B. Covelo, R. Kivekas and R. Sillanpaa, *Inorg. Chem*., 2007, **46**, 7818–7826.
28 J. G. Melnick, K. Yurkerwich, D. Buccella, W. Sattler and G. Parkin, *Inorg. Chem*., 2008, **47**, 6421–6426.
29 S. Park, S. Y. Lee and S. S. Lee, *Inorg. Chem*., 2010, **49**, 1238–1244.
30 A. Morsali and M. Y. Masoomi, *Coord. Chem. Rev*., 2009, **253**, 1882–1905.
31 a) A. A. Khandar, V. T. Yilmaz, F. Costantino, S. Gumus, S.A. Hosseini-Yazdia and G. Mahmoudi, *Inorg. Chim. Acta*, 2013, **394**, 36–44; b) M. Akkurt, A. A. Khandar, M. N. Tahir, S. A. Hosseini-Yazdi and G. Mahmoudi, *Acta Cryst.*, 2012, **E62**, m903–m904.

32 a) J. Lewiński, J. Zachara, I. Justyniak and M. Dranka, *Coord. Chem. Rev*., 2005, **249**, 1185-1199; b) M. Sakamoto, K. Manseki, H. Okawa, *Coord. Chem. Rev*. 2001, **219-221**, 379–414; c) H. Wang, W Cao, T. Liu, C. Duan and J. Jiang, Chem. Eur. J. 2013, **19**, 2266–2270, d) Q. Ma, X. Feng , W. Cao , H. Wang and J. Jiang, *CrystEngComm*, 2013, **15**, 10383–10388; e) H. Wang, D. Zhang, Z.-H. Ni, X. Li, L. Tian and J. Jiang, *Inorg. Chem*., 2009, **48**, 5946–5914

33 A. J. Bloodworth, *J. Organomet. Chem*., 1970, **23**, 27–30.

34 Z. Otwinowski and W. Minor, in Methods in Enzymology, Vol. 276, Macromolecular Crystallography, Part A, C. W. Carter Jr. and R. M. Sweet (Eds.), pp. 307-326. New York: Academic Press, 1997.

35 Bruker, APEX2, Bruker AXS Inc., Madison, WI, USA, 2004.

36 Oxford Diffraction, CrysAlis CCD and CrysAlis RED. Version 1.170. Oxford Diffraction Ltd, Wroclaw, Poland 2003.

37 G. M. Sheldrick, SADABS, Programs for Scaling and Correction of Area detection Data, University of Göttingen: Göttingen (Germany), 1996.

38 G. M. Sheldrick, *Acta Cryst*., 2008, **A64**, 112.

39 L. J. Farrugia, *J. Appl. Cryst*, 1999, **32**, 837.

40 R. Ahlrichs, M. Bär, M. Haser, H. Horn and C. Kölmel, *Chem. Phys. Lett.*, 1989, **162**, 165–169.

41 S. F. Boys and F. Bernardi, *Mol. Phys.* 1970, **19**, 553–566.

42 R. F. W. Bader, *Chem. Rev.* 1991, **91**, 893–928.

43 AIMAll (Version 13.11.04), T. A. Keith, TK Gristmill Software, Overland Park KS, USA **2013**.

44 S. G. Telfer and R. Kuroda, *Coord. Chem. Rev*., 2003, **242**, 33–46.

45 A. Blagus, D. Cinčić, T. Friščić, B. Kaitner and V. Stilinović, *Mac. J. Chem. Chem. Eng.*, 2010, **29**, 117–138.

46 F. H. Allen, O. Kennard, D. G. Watson, L. Brammer and A. G. Orpen, *J. Chem. Soc. Perkin Trans II*, 1987, S1–S19.

47 M. G. B. Drew, S. De and D. Datta, *Inorg. Chem. Acta*, 2009, **362**, 2487–2491.

48 V. Stilinović, D. Cinčić and B. Kaitner, *Acta Chim. Slov.*, 2008, **55**, 874–879.

49 a) H. B. Burgi, J. D. Dunitz and Eli. Shefter, *J. Am. Chem. Soc*., 1973, **95**, 5065–5067 b) J. Lewiński, W. Bury and I. Justyniak, *Eur. J. Inorg. Chem*. 2005, 4490–4492.

50 a) A. Bauzá, T. J. Mooibroek and A. Frontera, *Chem. Commun*., 2015, **51**, 1491–1493. b) A. Bauzá, R. Ramis and A. Frontera, J. Phys. Chem. A, 2014, **118**, 2827–2834.

TOC graphic

We report the synthesis and X-ray characterization of six neutral mercury(II) complexes of benzilbis((pyridin-2-yl)methylidenehydrazone or benzilbis((acetylpyridin-2-yl)methylidenehydrazone) and halide coligands.